Static and Dynamic Properties of Cross-Linked Poly(dimethylsiloxane) Pregel Clusters

M. Adam*,† and D. Lairez

Laboratoire Léon Brillouin CEA-CNRS, CEA-Saclay, 91191 Gif-sur-Yvette Cedex, France

M. Karpasas and M. Gottlieb

Chemical Engineering Department, Ben Gurion University, Beer Sheva 84105, Israel

Received February 10, 1997; Revised Manuscript Received June 19, 1997⊗

ABSTRACT: Experimental results concerning end-linked poly(dimethylsiloxane) pregel clusters quenched at different distances from the gelation threshold are reported. Static and quasielastic light scattering experiments and intrinsic viscosity measurements allow us to verify that static properties of this chemical system are properly described by the percolation model. The critical behavior of the rheological properties is investigated with particular attention to the temperature and concentration dependence of the exponent values. It is shown that in this chemical system, local dynamic properties are independent of the distance to the threshold, allowing "real" exponents to be evaluated. One finds that the exponents governing the divergence of the viscosity, *s*, the emergence of the elastic modulus, *t*, and the frequency dependence of the elastic modulus, *u*, are equal to $s = 1.1 \pm 0.06$, $t = 1.9 \pm 0.15$, and $u = 0.69 \pm 0.005$.

Introduction

The de Gennes[1] and Stauffer[2] challenge concerning the pertinence of percolation to the description of gelation within the framework of scaling laws is 2-fold: the static properties (growth and conformation) of polymer clusters and the dynamic (mechanical) behavior of these clusters. The former has been fully verified experimentally,[3] while the latter is the obscure part of the challenge. In order to account for the mechanical properties, a hypothesis on the type of interaction between polymer clusters has to be made in addition to the scaling assumptions. A recent review[3] of theoretical expectations and experimental results, allows us to be very concise here in the account of previous work. One of the conclusions in this review was that experimental results do not help in clarifying the problem of dynamic behavior, because exponent values are widely scattered and depend on the details of the chemical system studied. On the other hand, scaling behavior for the dynamic properties of chemical gels was never clearly established. It was previously shown,[4] for branched polyurethane clusters near the gelation threshold, that the scaling failure is due to local properties which depend on the distance from the threshold. More particularly for this system, only "apparent" exponent values, concentration and temperature dependent, are determined. For example the exponent *s* governing the divergence of the viscosity as the gelation threshold is approached, is equal to 1.4 and 1.63 at 70 and 20 °C, respectively. The present paper is concerned with the study of a chemical system prepared of end-linked poly(dimethylsiloxane) (PDMS) which is found to be free of these complications.

In the first part, we recall the theoretical expectations from the percolation theory applied to polymer clusters near the gelation threshold. In the Experimental Section, we report static and dynamic light scattering experiments as well as intrinsic viscosity measurements, performed on nonstoichiometric PDMS pregel, elaborated at different distances from the gel point. Once the relevance of percolation theory and its ability to describe the static properties of this chemical system has been verified, we focus our attention on the dynamic properties of the polymer.

1. Theoretical Predictions

1.1. Static Properties. In the vicinity of the gelation threshold, the mass distribution of the polymer clusters is described by a power law of the form[2,3,5]

$$n \propto M^{-\tau} f\left(\frac{M}{M^*}\right) \qquad \text{with} \qquad \tau = 2.2 \tag{1}$$

where n is the number of clusters with mass M and $f(M/M^*)$ is the cutoff function indicating that there is no mass larger than M^* in the system. The mass M^* and the size ξ of the largest polymer cluster are linked by

$$M^* \propto \xi^D \tag{2}$$

This relation, which expresses the fractal conformation of the largest cluster, is actually valid for all clusters of size R such that $M \propto R^D$. The value of the fractal dimension D depends on the polymer environment: (i) in the reaction bath (without solvent) $D = D_p = 2.5$ and (ii) in dilute solution,[6] due to the polymer cluster swelling $D = D_s = 2$.

Scattering experiments give access to the weight average molecular weight M_w, to the *z*-average square radius of gyration $\langle R_g^2\rangle_z$, and to the *z*-average diffusion coefficient $\langle \mathbf{D}\rangle_z$ of polymer clusters:

---

† Present address: Institut Laue Langevin, BP 156, 38042 Grenoble Cedex 9, France.

⊗ Abstract published in *Advance ACS Abstracts,* August 15, 1997.

S0024-9297(97)00184-8 CCC: $14.00

$$M_w = \frac{\sum_1^{M^*} n_i M_i^2}{\sum_1^{M^*} n_i M_i}, \qquad \langle R_g^{\,2}\rangle_z = \frac{\sum_1^{M^*} n_i M_i^2 R_{gi}^{\,2}}{\sum_1^{M^*} n_i M_i^2},$$

$$\langle \mathbf{D}\rangle_z = \frac{\sum_1^{M^*} n_i M_i^2 \mathbf{D}_i}{\sum_1^{M^*} n_i M_i^2} \qquad (3)$$

Making use of the mass distribution law (eq 1), these quantities are found to be linked by

$$M_w \propto R_z^{\,(3-\tau)D} \qquad (4)$$

R_z is either the radius of gyration R_{gz} $(=\sqrt{\langle R_g^{\,2}\rangle_z})$ or the hydrodynamic radius deduced from the diffusion coefficient $\mathbf{D}_z$. Both radii are proportional.[7] The exponent D is either D_s or D_p depending on the experimental conditions. In the reaction bath, R_z is proportional to ξ, the size of the largest cluster. The weight average molecular weight diverges toward the gel point as

$$M_w \propto \epsilon^{-\gamma} \qquad \text{with} \qquad \gamma = 1.74 \qquad (5)$$

where ϵ is the relative distance to the threshold. If p is the fraction of reacted bonds and p_c its value at the threshold, then $\epsilon = |(p - p_c)/p_c|$.

In solution at the overlap concentration C^*, the entire set of polydisperse polymer clusters is in closed packing condition.[8] Thus, the total volume occupied by all the polymer clusters is equal to the overall volume of the solution. Hence

$$C^* \propto M_w^{\,-X} \qquad \text{with} \qquad X = \frac{3}{(3-\tau)}\left(\frac{1}{D_s} - \frac{1}{D_p}\right) = 0.375 \qquad (6)$$

C^* is inversely proportional to the interaction parameter B_w. If we accept the assumption that diluted polymer clusters are subjected to hydrodynamic interactions, C^* is also predicted[9] to be inversely proportional to the intrinsic viscosity, defined as $[\eta] = \lim_{C\to 0}((\eta_{rel} - 1)/C)$, where the relative viscosity η_{rel} defined as the viscosity of the polymer solution η of concentration C divided by the solvent viscosity η_s. One has to note that if polymer clusters do not swell under dilution ($D_s = D_p$), then C^*, B_w, and $[\eta]$ are expected to be independent of M_w. Thus, dependence of these properties on the molecular weight is an indication of cluster swelling.

Within critical phenomena theory, a universality class is defined by two independent exponent[10] values, the others being deduced by scaling and hyperscaling laws. Thus, only two exponent values have to be determined experimentally in order to verify that the percolation model describes adequately the growth and conformation of the PDMS polymer clusters.

1.2. Dynamic Properties. As a system undergoes a sol−gel transition, it transforms from a viscoelastic liquid into a viscoelastic solid state. In other words, the zero shear macroscopic viscosity η diverges below the threshold as

$$\eta = \eta_0 \epsilon^{-s} \qquad (7)$$

while the zero frequency elastic modulus, G, increases above the threshold as

$$G = G_0 \epsilon^{t} \qquad (8)$$

where η_0 and G_0 are local properties, which are expected to be independent of the relative distance to the gel point ϵ. At frequencies higher than the inverse of $\mathbf{t}^*$, the relaxation time of the largest cluster, scaling laws imply that the complex shear modulus G^*, is independent of the mass of the largest cluster and thus independent of ϵ. One can show[1,11] that, for frequencies ω smaller than the characteristic cutoff glass transition frequency (ω_0) but higher than $1/\mathbf{t}^*$ ($\omega_0 > \omega > 1/\mathbf{t}^*$)

$$G^*(\omega) = (G_0/\omega_0^{\,u})\omega^u e^{iu(\pi/2)} \qquad \text{with} \qquad u = t/(s + t) \qquad (9)$$

The loss angle tangent ($\tan \delta$), which is the ratio G''/G' of the imaginary part to the real part of the elastic modulus, is then independent of the frequency and of the relative distance to the threshold. Relation 9 can be written in the scaling form, valid at any frequency domain:

$$G^*(\omega \mathbf{t}^*) = GF(i\omega \mathbf{t}^*) \qquad (10)$$

with $F(i\omega\mathbf{t}^*) \propto \omega^u$ for $\omega_0 > \omega > 1/\mathbf{t}^*$ and G the zero frequency elastic modulus (eq 8). The characteristic time $\mathbf{t}^*$ follows:

$$\mathbf{t}^* = (1/\omega_0)\epsilon^{-(s+t)} \qquad (11)$$

In the time domain, the counterpart of eq 9 for times shorter than $\mathbf{t}^*$ (but larger than t_0) is

$$\eta(t) = \eta t^{-(1-u)} \qquad (12)$$

For $t/\mathbf{t}^* > 1$, the reduced relaxation spectrum $\eta(t)/\eta$ becomes dependent on ϵ because the relaxation is sensitive to the size of the largest polymer cluster. Even in this time domain, one may account for this dependence by using the reduced variables $\eta(t)/\eta$ as a function of $t/\mathbf{t}^*$. Note that the former equations, related to the dynamic properties, result from scaling assumptions; thus they are theoretically independent of the nature of hydrodynamic interactions between polymer clusters. It is only the exponent values that depend on the type of interactions.

Rouse model[12] (without hydrodynamic interaction):
$s = 4/3$, $t = 8/3$, $u = 2/3$

electrical/mechanical analogy:[13]
$s = 0.75$, $t = 1.9$, $u = 0.72$

As pointed out in the Introduction, the exponent values s and t, determined by different authors, are widely scattered.[3] The purpose of this work is to determine the two dynamic exponent values on a chemical system for which local dynamics are temperature and concentration independent.

2. Experimental Procedures

2.1. Chemical Synthesis. The cross-linked polymers used in this study were prepared by a reaction between vinyl terminated linear PDMS and a four functional silane cross-linker. The prepolymer and cross-linker were obtained from Petrarch Systems (presently United Chemical Technologies, Inc. Bristol, PA). Oligomers and low molecular weight contaminants were removed from the polymer by vacuum stripping. The molecular weight of the prepolymer, $M_n = 4900$, was determined by vapor pressure osmometry (Knauer) and by size exclusion chromatography (a 4 column Waters with RI detector) using PDMS standards for calibration. The functionality of the polymer was verified by NMR end-group analysis and found to be better than 98%. The cross-linker used was tetrakis(dimethylsiloxy)silane [$(HSiMe_2O)_4Si$] with nominal molecular weight $M = 328.7$. By GC/MS analysis it was found to be composed of four major components with at least 99.8% hydrosilane material and with $M_n = 342$ and effective functionality of 3.87 (instead of the nominal 4). The material was used as received.

The quenched pregel samples were prepared in bulk by using a nonstoichiometric mixture of the components always using cross-linker-poor compositions to minimize the danger of parasitic reactions involving the silane groups. The cross-linked samples were prepared by thoroughly mixing in a 10 mL vial half the appropriate amount of the degased prepolymer and all the cross-linker required to achieve the final desired value of r (<1), the stoichiometric ratio of reactants (defined as the ratio of initial molar concentration of silane groups to that of vinyl groups: $r = [SiH]_0/[Vi]_0$). The second half of the prepolymer was mixed with approximately 5 μL of catalyst solution, and finally, the two parts were combined in the vial and thoroughly mixed again. The vial was placed on a roller mixer and allowed to react for 48 h at room temperature followed by 24 h postcure at 60 °C. The catalyst solution used was a 2% platinum complex (*cis*-dichlorobis(diethyl sulfato)platinum(II)) in toluene. The reaction is usually completed at room temperature within 4 h as judged by the complete disappearance of the SiH peaks in FTIR spectra of reaction mixtures. The reticulation was formed in bulk by the hydrosilation reaction:

$$\equiv Si-CH=CH_2 + HSi\equiv \xrightarrow{Pt} \equiv Si-CH_2-CH_2-Si\equiv$$

The evolution of structure in this system is well characterized, and the chemistry of its cure has been studied extensively.[14] The extent of side reactions of the hydride silane groups on the cross-linker was found to be negligible under the conditions used here. The experimental critical stoichiometric ratio to obtain gelation r_c was determined by flow/dissolution tests and found at $r_c = 0.335 \pm 0.01$.This is within experimental accuracy from the theoretical value, indicating side reactions and loop-forming intramolecular reactions do not play an important role in the present case. In spite of this, the value of r_c has not been used in this work since large errors in the estimation of critical exponents are introduced when relying only on the distance to the threshold for their evaluation. This is due to the great sensitivity of exponent value on slight change in r_c on one hand and to the limited experimental accuracy on the exact gel point on the other. A total of 15 samples with different $r < r_c$ (i.e., quenched at different distances below the critical threshold) and one sample above the threshold were prepared.

2.2. Intrinsic Viscosity. Polymer samples were dissolved in toluene, and the concentration was determined by weighing. The viscosities of the polymer solutions were measured with a range of Cannon-Fenske semi-micro capillary viscometers (Cannon Instrument Co., State College, PA). Different diameters were selected to obtain the proper efflux times (>100 s) such that kinetic energy corrections are not required. The effect of shear rate was examined by the use of a narrower capillary. The difference in [η] values was insignificant.

The viscometer was suspended in a thermostatically controlled water bath maintained at the required temperature to within ±0.2 °C. Equilibration time of 15−20 min was allowed before measurements were made since the solution in the viscometer was experimentally found to reach thermal equilibrium within 10 min.

The relative viscosity of a given solution η_{rel} was determined by measurement of the relative efflux times in the capillary. Viscosity values were based on at least 2−3 efflux time readings taken for any given sample inserted into the viscometer. Variation between consecutive readings was lower than 1.5% and typically around 0.5%. At least two independent viscosity determinations were performed for each concentration. Five to seven experimental points were used for extrapolation to obtain the intrinsic viscosity [η]. The intrinsic viscosity is obtained from the combined extrapolation of $\ln(\eta_{rel}/C)$ (Kraemer relation) and $(\eta_{rel} - 1)/C$ (Huggins relation) to zero polymer concentration C. Failure of the two extrapolations to coincide resulted in rejection of the data.

2.3. Light Scattering. The home made apparatus as well as the data reduction procedure were described elsewhere.[15] The incident wavelengths used are either $\lambda = 488$ or 647 nm. The transfer vector $q = (4\pi n/\lambda)\sin(\theta/2)$ varies between 1.5×10^{-3} and 3.7×10^{-2} nm^{-1}, where n is the refractive index and θ is the scattering angle. Samples were dissolved in toluene, the solution concentration being determined by weighing. In order to eliminate dust particles, the solutions were either filtered on 0.45 μm Millipore filter or centrifuged in the case of samples having a weight average molecular weight higher than 2×10^6 to prevent the largest polymer clusters from being eliminated by filtration. Let us recall the different quantities light scattering experiments allow us to measure.

The weight average molecular weight M_w is obtained from double extrapolation of the scattered intensity per monomer to zero q and zero concentration:

$$\left(\frac{I_{q\to 0}}{C}\right)_{C\to 0} = KM_w \tag{13}$$

where I is the ratio of the polymer to the solvent scattered intensity. The constant K depends on the wavelength λ, the Rayleigh ratio of the solvent (toluene), the refractive index, and its increment with polymer concentration. Its values are $K = 5.65 \times 10^{-3}$ and 5.28×10^{-3} (cm^3 mol)/g^2 for $\lambda = 488$ and 647 nm, respectively.

The interaction parameter B_w is determined by the concentration dependence of the zero q scattered intensity per monomer:

$$\left(\frac{I_{q\to 0}}{C}\right) = \left(\frac{I_{q\to 0}}{C}\right)_{C\to 0}(1 - 2B_wC + ...) \tag{14}$$

The z-average radius R_z is determined by extrapolation of the radius of gyration R_{gz} and/or the hydrodynamic radius R_{Hz} to zero concentration. The radius of gyration is obtained from the q dependence of the scattered intensity for $qR_{gz} < 1$:

$$\frac{i}{C} = \frac{I_{q\to 0}}{C}\left(1 - \frac{q^2 R_{gz}^{\ 2}}{3} + ...\right) \tag{15}$$

The hydrodynamic radius R_{Hz} is extracted from the diffusion coefficient $\mathbf{D}_z$ by making use of the Stokes−Einstein relation:

$$\mathbf{D}_z = \frac{kT}{6\pi\eta_{loc}R_{Hz}} \tag{16}$$

where k the Boltzmann constant, T is the temperature, and η_{loc} is the local viscosity expected to be, in dilute solutions, close to the solvent viscosity. The diffusion coefficient in turn, is measured through the dynamic form factor: $S(q,t) = \exp(-(\mathbf{D}q^2t)^{\beta})$. For $qR_{gz} < 1$, $\beta = 1$, and the measured diffusion coefficient is independent of q. The ratio R_{Hz}/R_{gz} is equal to $0.56R_H/R_g$, where the constant 0.56 comes from integration constant[7] with $D = 2$ and $\tau = 2.2$ and the ratio R_H/R_g stands for monodispersed branched polymers.

For the given set of samples quenched at different distances from the gelation threshold M_w, R_z, and B_w are obtained individually for each sample by the light scattering data reduction procedures described above (eqs 13−16). Note that these equations all require data obtained in dilute solutions ($C/C^* < 1$) and at small reduced transfer vector ($qR_{gz} < 1$). The B_w−M_w and R_z−M_w dependencies of the entire set of samples allow the experimental determination of the exponents X (eq 6) and $(3 - \tau)D_s$ (eq 4).

In addition, the value of the latter exponent may also be determined from data on an individual sample by examination of the q dependence of the scattered intensity at large reduced transfer vector ($qR_{gz} > 1$). The scattered light intensity may be written as the product of two quantities: $I(q)/C = M_w f(qR_z)$. At short length scale, ($qR_{gz} > 1$) scattered intensity is not sensitive to the overall size or mass of the polymer cluster and thus should be independent of M_w. Hence, the function $f(qR_z)$ is a power law such that[16] $I(q)/C = q^{-(3-\tau)D_s}$. Using similar arguments, we may examine the diffusion coefficient obtained by quasielastic light scattering at short length scales ($qR_{gz} > 1$) as opposed to the large length scale ($qR_{gz} < 1$) data analysis described in conjunction with eq 16. For $qR_{gz} > 1$ the q dependence of the diffusion coefficient can be written, as for the static properties, using a scaling law: $\mathbf{D}(q) = \mathbf{D}_{q\to 0}\, f(qR_{gz})$ with $\mathbf{D}_{q\to 0} \propto 1/R_{Hz}$ and the function $f(qR_{gz})$ is a power law such that $\mathbf{D}(q)$ is independent of R_{gz} at $qR_{gz} > 1$ (to contrast with $\mathbf{D}$ independent of q at large length scales). This leads to a q-dependent diffusion coefficient $\mathbf{D}(q) = (kT/6\pi\eta_{loc})q$, independent of the polydispersity contrary to static properties. The latter linear q relation is derived on the assumption that the two radii measured by static (R_{gz}) and by quasielastic (R_{Hz}) light scattering are related by a proportionality constant. The correctness of this assumption has been considered at length[13,17] for the case of linear monodisperse polymers in dilute solution of a good solvent. In that case, the ratio R_H/R_g, is found to be molecular weight dependent and the diffusion coefficient varies as $\mathbf{D}(q) \propto q^{0.9}$ for $qR_g > 1$. The deviation from the expected theoretical predictions is explained[18] in terms of the crossover between the Gaussian ($D = 2$) conformation for "short" chains and the self-avoiding walk ($D = 1.7$) for "longer" chains. The crossover between these two conformations occurs later for the dynamic properties because the excluded volume interactions are more efficient for static properties than for dynamic ones. It is only for very high molecular mass, or when the excluded volume is as efficient for static as for dynamic properties, that $\mathbf{D}(q)$ is proportional to q and the ratio R_H/R_g is a constant[19] equal to 0.64. This ratio, which can be measured directly from the extrapolation of the appropriate light scattering data, as previously explained, can also be deduced independently from the ratio of the intrinsic viscosity to the interaction parameter B_w:

$$\frac{R_{Hz}}{R_{gz}} \propto \frac{[\eta]}{B_w} \qquad (17)$$

2.4. Rheological Properties. Viscosity η and time-dependent relaxation spectrum η(t) are measured using the magnetorheometer,[20] the components of the complex dynamic shear modulus G' and G'' are measured on a constant stress rheometer. The magnetorheometer is a homemade apparatus allowing polymers to be studied in a volatile solvent. Experiments consist of measuring the magnetic force needed for a levitating magnetic sphere of radius r to remain at a fixed spatial position while a step motor sets the surrounding liquid in motion at a constant velocity v. The steady viscosity η is deduced from the ratio of the measured stress σ (proportional to the magnetic force) to the shear rate $\dot{\gamma} = v/r$. In order to ensure that the measured viscosity is actually Newtonian, i.e. independent of $\dot{\gamma}$, we check that the viscosity is constant within experimental precision (2%) as the velocity is varied by a factor 10. The time-dependent relaxation spectrum η(t) is obtained from the measured relaxation of the magnetic force σ(t) recorded after the cessation of the imposed steady shear flow under constant shear rate $\dot{\gamma}$. The time dependent viscosity can thus be determined by the ratio $\eta(t) = \sigma(t)/\dot{\gamma}$. As one expects a power law behavior for the stress relaxation spectrum, the magnetic force was recorded using up to eight time windows.

The dynamic moduli of the samples were determined on a Carrimed CLS100 constant stress rheometer using 4 and 6 cm parallel plates and 100 μm gap at 25 °C. Frequency scans were carried out at the lowest stress possible to avoid sample damage. The linearity of the response was constantly monitored to ascertain linear viscoelasticity. The upward frequency sweep covering the range from 0.01 Hz (the lowest reproducible deformation for the most elastic material) to 40 Hz (the highest accessible frequency) was followed by a downward sweep on the same sample. In all samples upward and downward frequency sweeps overlaid with not observable deviations.

Table 1. Sample Characteristics: Weight Average Molecular Weight M_w, z-Average Radius of Gyration R_{gz}, z-Average Hydrodynamic Radius R_{Hz}, Weight Average Interaction Parameter B_w, Intrinsic Viscosity $[\eta]$, and Macroscopic Viscosity η Measured at $T = 20$ °C[a]

$M_w \times 10^{-5}$	R_{gz} (nm)	R_{Hz} (nm)	B_w (cm^3/g)	$[\eta]$ (cm^3/g)	η (p)
1.78	23.0	15.0	32.4	15.9	11.0
1.89	26.6	15.5	27.7	16.0	11.1
2.43	30.8	19.3	38.2	16.6	13.6
2.83	38.5	17.1	43.3		13.6
3.23	41.4	25.2	36.4	16.9	17.0
4.14	50.2	30.8	37.7	17.5	21.3
4.6	48.3	26.5	49.6		18.4
4.94	51.5	33.4	47.5	17.9	22.0
6.7	58.2	33.4	54.0	18.5	22.1
7.76	68.0	42.8	48.4	19.4	26.1
10.8	77.7	50.8	55.7	20.1	31.1
16.4	91.0	56.2	82.0	22.7	38.7
22.9	124	69.3	84.4	24.4	52.3
74.3	235	120	102	25.8	111
206	373	267	162	31.5	220

[a] Precision on the different quantities measured are of the order of 3%.

3. Experimental Results

The experimental results are listed in the Table 1. For each sample are listed values of the weight average molecular weight (M_w), the z average radius of gyration (R_{gz}), and the interaction parameter B_w obtained from static light scattering, the hydrodynamic radius (R_{Hz}) obtained from quasielastic light scattering, and the intrinsic viscosity $[\eta]$ and the zero shear rate viscosity (η) obtained by the magnetorheometer at 20 °C. The relative distance to the threshold is not listed because no use is made of it. We circumvent the difficult problem of the accurate determination of the gelation threshold by considering the variations of the different quantities measured only as a function of the independently measured weight average molecular weight. Thus, only exponent ratios will be determined.

3.1. Conformation of Polymer Clusters in Dilute Solutions. For all the samples, we find the ratio of the two radii R_{Hz}/R_{gz} to be constant such that

$$R_{Hz}/R_{gz} = 0.61 \pm 0.05 \qquad (18)$$

One can compare this numerical factor to the integration constant (see comments following eq 16 and ref 7). The agreement between those two values (0.61 and 0.56) could indicate that the R_H/R_g ratio of monodisperse branched polymer is of the order of 1. In Figure 1, the weight average molecular weight is plotted in double logarithmic scales as a function of the z-average radius R_z. The radius R_z is either taken as the hydrodynamic radius R_{Hz} (full points) or, on the basis of eq 18, as $0.61R_{gz}$ (empty points). The straight line in Figure 1 is the best fit of the data. The exponent value obtained from the slope of this line is equal to

$$(3 - \tau)D_s = 1.71 \pm 0.07 \qquad (19)$$

As explained above, the exponent $(3 - \tau)D_s$ can be obtained either from the small q data ($qR_{gz} < 1$) of all the samples collectively, as done in eq 19 or from the

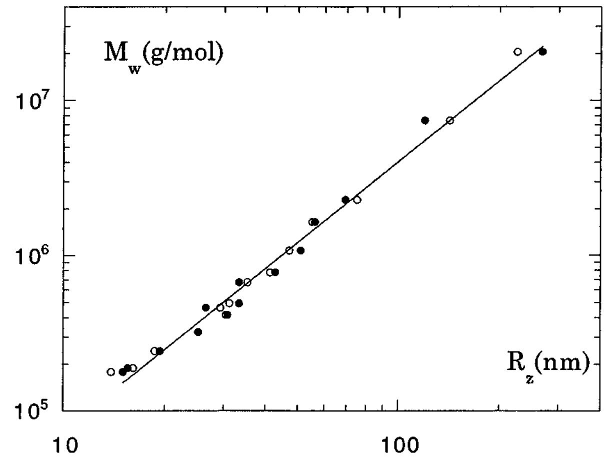

Figure 1. Log–Log plot of the weight average molecular weight M_w as a function of the z-average radii R_z. R_z stands for the z-average hydrodynamic radius R_{Hz} (●) or $0.61R_{gz}$ (○) where R_{gz} is the z-average radius of gyration (see text and eq 18). The straight line corresponds to the best fit: $M_w = 1400R_z^{1.71}$, leading to $(3 - \tau)D_s = 1.71$.

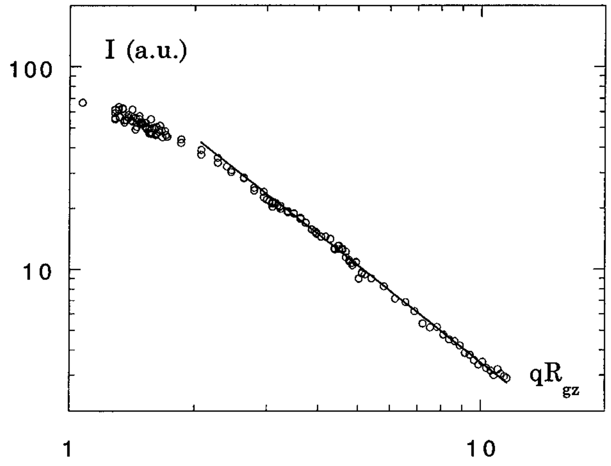

Figure 2. Log–Log plot of the scattered intensity I as a function of the reduced transfer vector qR_{gz}. The radius of gyration R_{gz} (320 nm) is deduced from the low q values part of this curve. The sample characteristics are $M_w = 2.06 \times 10^7$, $C = 1.1 \times 10^{-3}$ g/cm^3. The straight line has a slope equal to 1.59 corresponding to the exponent $(3 - \tau)D_s$ determined for $2.5 < qR_{gz} < 11.5$.

large q data ($qR_{gz} > 1$) of a single sample. Thus, for one sample ($M_w = 2.06 \times 10^7$) at one given concentration (C(g/cm^3) $= 1.1 \times 10^{-3}$) the q dependence of the scattered intensity at $qR_{gz} > 1$ (see Figure 2) yields $(3 - \tau)D_s = 1.57 \pm 0.06$. However, this exponent is found to depend on polymer concentration with increasing values for decreasing concentration. By repeating the experiment on the same polymer sample at different concentrations, the limiting slope d Log(I)/d Log(q) is measured at $q > 1.5 \times 10^{-2}$ nm^{-1} (see Figure 3). Extrapolation to zero concentration leads to

$$(3 - \tau)D_s = 1.64 \pm 0.06 \qquad (20)$$

This value is within experimental precision, in agreement with the value determined for the whole set of samples (eq 19) and with the theoretical prediction $(3 - \tau)D_s = 1.6$. The agreement between eqs 19 and 20 is an endorsement of the polymers self-similarity. Thus from this point of view, it indicates that polymer clusters are formed by a random reticulation process and proves the samples quality as far as chemistry is concerned.

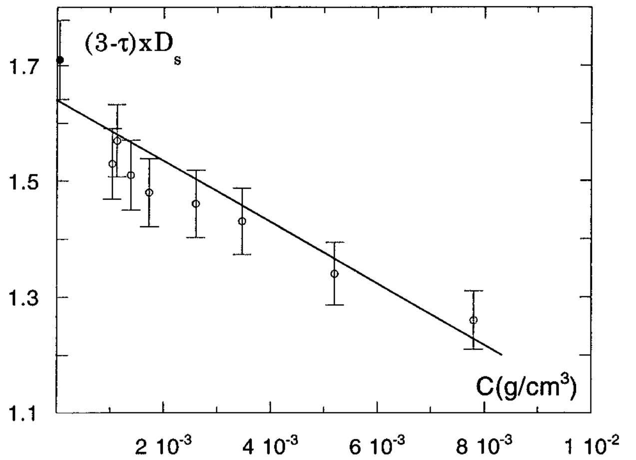

Figure 3. Variation of the exponent value $(3 - \tau)D_s$ with the concentration C. Exponent values are deduced from the limiting slope d(log(I))/d(log(q)) measured at $q > 1.5 \times 10^{-2}$ nm^{-1}, on dilute solutions for the highest molecular weight sample ($M_w = 2.06 \times 10^7$, empty circles). The filled circle corresponds to the exponent value deduced from the variation of M_w as a function of R_z (Figure 1, eq 19) measured on the entire set of different samples. (The straight line serves only as a guide for the eyes passing through the error bars.)

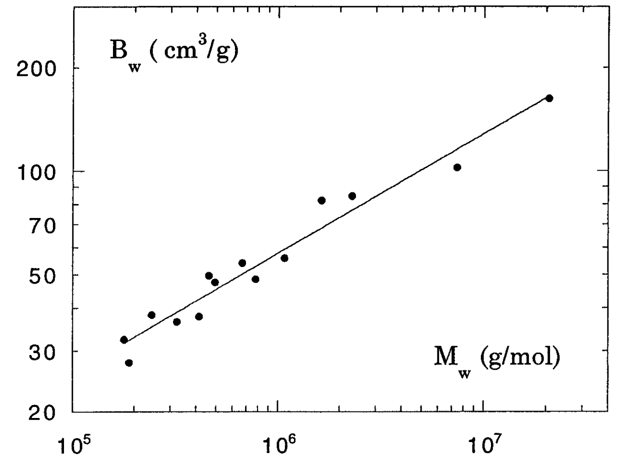

Figure 4. Interaction parameter B_w as a function of the weight average molecular weight M_w. The graph is in Log–Log scale and the slope of the straight line corresponds to the exponent $X = 0.35$ (eq 21).

The interaction parameter B_w is found to depend on the weight average molecular weight, which confirms that these polymer clusters swell upon dilution (cf. discussion following eq 6). In Figure 4 the straight line corresponds to

$$B_w = 0.47 M_w^{X} \quad \text{with } X = \frac{3}{(3 - \tau)}\left(\frac{1}{D_s} - \frac{1}{D_p}\right) = 0.35 \pm 0.03 \qquad (21)$$

This exponent value is in good agreement with the theoretical prediction ($X = 0.375$, see eq 6).

In Figure 5 the ratio of the intrinsic viscosity to the interaction parameter, $[\eta]/B_w$, is plotted as a function of the weight average molecular weight. This ratio decreases as the molecular weight increases (empty points), and it is not proportional to the ratio of the z-average radii R_{Hz}/R_{gz} (full points) as speculated by eq 17. The M_w dependence of $[\eta]$ does not agree with eq 6 and the discussion following it. The fact that R_{Hz}/R_{gz} is independent of the weight average molecular weight indicates that excluded volume interactions are as

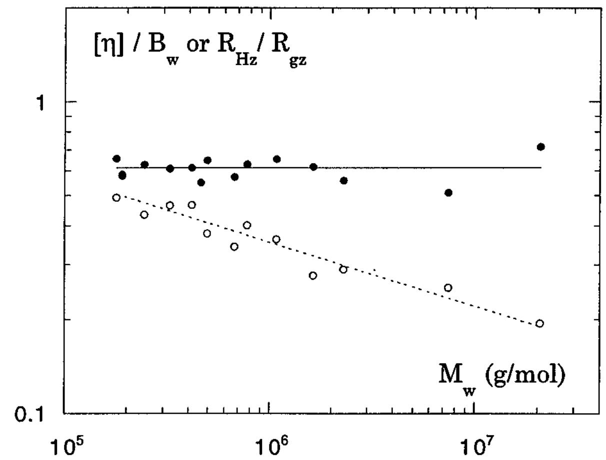

Figure 5. Ratio of the intrinsic viscosity to the interaction parameter $[\eta]/B_w$ (○) is molecular weight-dependent while the ratio of the two z-average radii R_{Hz}/R_{gz} (●) is independent of the molecular weight. The dotted line corresponds to the best fit of $[\eta]/B_w \propto M_w^{-0.2}$, while the full line corresponds to the mean value $R_{Hz}/R_{gz} = 0.61$. Both quantities were expected to be proportional (cf. eq 17).

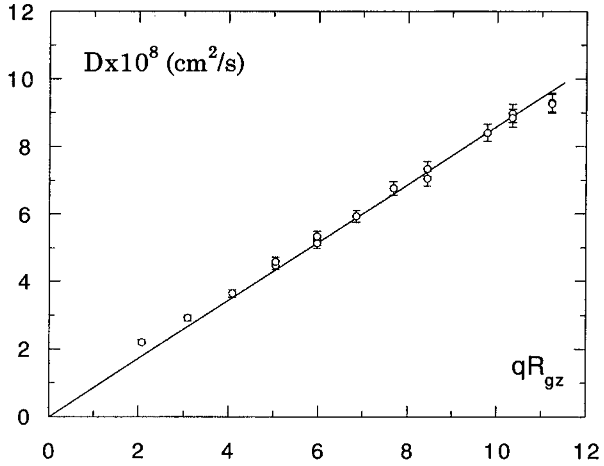

Figure 6. Diffusion coefficient $\mathbf{D}(q)$ measured by quasielastic light scattering as a function of the reduced transfer vector qR_{gz}. The sample characteristics are $M_w = 2.06 \times 10^7$, $R_{gz} = 310$ nm, and $C = 2.3 \times 10^{-3}$g/cm^3. A linear behavior characteristic of internal modes is found.

efficient for static as for dynamic properties for the size of polymer clusters tested here. Thus the dependence of $[\eta]/B_w$ on molecular mass stems from the fact that the mean size accessible by scattering experiments (from which B_w is obtained) is different from the mean value accessible by intrinsic viscosity experiments.

The dynamic form factor $S(q,t)$ was measured by quasielastic light scattering on one of the diluted samples ($M_w = 2.06 \times 10^7$) at $2 < qR_{gz} < 11$. In this q range the dynamic form factors measured at different scattering angles lie on a single curve using tq^3 as variable. They can be fitted properly by using a stretched exponential decay with an exponent equal to $\beta = 0.77 \pm 0.02$. The diffusion coefficient $\mathbf{D}(q)$, deduced from the measured characteristic decay time, varies linearly with q (see Figure 6). It is, as expected, independent of the polydispersity. The local viscosity $\eta_{loc} = kTq/(6\pi\mathbf{D}(q))$ is found to be higher than the solvent viscosity by a factor of (1.46 ± 0.03), in agreement with the factor $(1.35)^{3/2} = 1.57$ predicted theoretically[21] and with the factor 1.5 found experimentally[22] for linear polymers.

So far, two independent exponent values related to the conformation of swollen polymer clusters have been determined (eqs 19 or 20 and 21). They are found to have values close to the values expected by the percolation model. Moreover, on a very similar system (end-linked linear PDMS[23]) the exponent τ was measured by size exclusion chromatography and found to be equal to $\tau = 2.27 \pm 0.04$, a value consistent with the values obtained here. The static properties of end-linked poly(dimethylsiloxane) polymer clusters being in agreement with the percolation model let us focus on the viscoelastic properties.

3.2. Dynamic properties. 3.2.1. Zero Shear Viscosity.

If the temperature and concentration dependence of the macroscopic viscosity are independent of the distance to the threshold, i.e., of the molecular weight M_w, then the viscosity can be expressed as a product of two independent functions: one $F(T,w)$ dependent on temperature and concentration, and the other $\eta(M_w)$ dependent on M_w:

$$\eta(M_w,T,w) = \eta(M_w)\,F(T,w) \qquad (22)$$

where w is the weight fraction of polymer (expressed in g/g) and $\eta(M_w)$ stands for $1/T = 0$ and $w = 1$. In order to study the scaling behavior of the viscosity, one needs to check first the actual independence of the two functions in eq 22 and then to concentrate on the behavior of $\eta(M_w)$.

For all the samples for which the temperature dependence of the viscosity was measured, an Arrhenius type dependence was observed, allowing us to describe the temperature dependence by an equation of the form

$$\eta(M_w,T,w) = \eta(M_w)\exp(E/kT) \qquad (23)$$

The fit of the measured viscosity as a function of the inverse temperature allows us to determine the prefactor $\eta(M_w)$ and the activation energy E/k. One finds $E/k = 1800 \pm 30$ K independent of the weight average molecular weight of the samples (see inset of Figure 7). In Figure 7, the ratio $\eta(M_w,T,w)/\eta(M_w)$ is plotted as a function of the inverse of the temperature for samples prepared at different distances to the threshold, clearly demonstrating the Arrhenius behavior.

As for the concentration dependence of the viscosity, in four samples ($2.8 \times 10^5 < M_w < 1.6 \times 10^6$) toluene was added to the polymer melt in small enough quantity ($0.5 < w$ (g/g) < 1) to ensure that polymer clusters remain in the interpenetrated regime ($B_wC > 20$). The viscosity was measured as function of concentration at constant temperature (20 °C). The concentration dependence of the viscosity for these samples samples can be successfully fitted by an expression of the form[24]

$$\eta(M_w,T,w) = \eta(M_w)\exp(Aw^2) \qquad (24)$$

where the concentration w is expressed in g/g. The parameter A depends slightly on the molecular weight increasing from 4.34 to 4.62 as M_w increases from 2.83×10^5 to 1.64×10^6 (see inset of Figure 8). As a first approximation, this modest variation is neglected and using a mean value of 4.5 for A in Figure 8, the ratio $\eta(M_w,T,w)/\eta(M_w) = F(w,T = 20\ °\mathrm{C}) = \exp(Aw^2)$ is plotted in Log scale as a function of the square of the concentration for the different samples. A single linear behavior is found for all the samples in support of the proposed analysis.

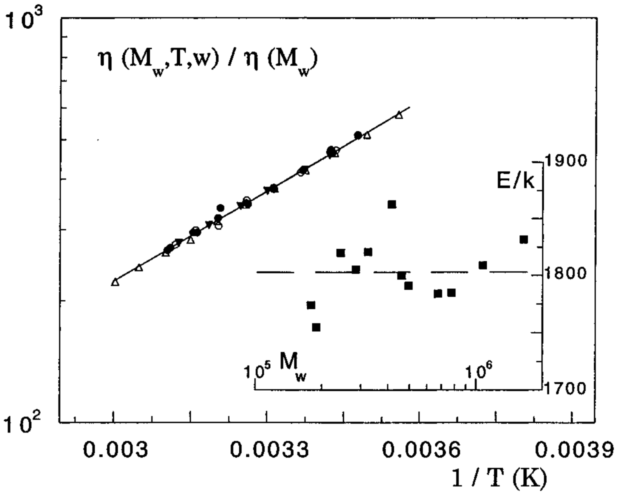

Figure 7. Variation of the viscosity with the inverse of the temperature. The viscosity $\eta(M_w,T,w)$, normalized by the prefactor of the Arrhenius law (eq 23), $\eta(M_w)$, is measured on different samples in the bulk (w = 1g/g). The temperature dependence of the normalized viscosity is found to be independent of the molecular weight M_w. The symbols ●, △, ▼, and ○, correspond to $M_w \times 10^{-5}$ = 2.83, 4.61, 6.73, 16.4, respectively. For the sake of clarity, and in order to compare with the concentration behavior, only results obtained on four samples are plotted. The full line corresponds to exp(1800/T). The ratio of the activation energy to the Boltzmann constant E/k (in K) is actually M_w independent (see the inset).

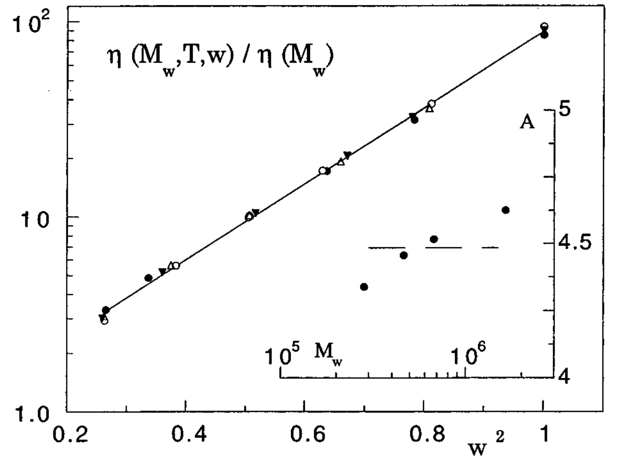

Figure 8. Variation of the normalized viscosity $\eta(M_w,T,w)/\eta(M_w)$, as a function of the square of the concentration w^2 for different samples at T = 20 °C (cf. eq 24). An exponential law is found which is M_w independent. The full line corresponds to exp(Aw^2) with A = 4.5, (symbols have the same meaning as in Figure 7). In the inset the quantity A is shown as a function of the molecular weight; the dotted line corresponds to the mean value: $A = 4.5 \pm 0.1$.

The results presented by eqs 23 and 24 confirm that $\eta(M_w,T,w)/\eta(M_w)$ is actually independent of M_w. Thus, the exponent extracted from the variation of the viscosity with the relative distance to the gel point is a "real" exponent rather than an "apparent" exponent, as was found on other systems.[4] At a given temperature (T = 20 °C) and a given concentration (w = 1g/g), the variation of the zero shear viscosity is studied as a function of the weight average molecular weight M_w (Figure 9). The exponent ratio s/γ is found to be equal to[25]

$$s/\gamma = 0.62 \pm 0.03 \qquad (25)$$

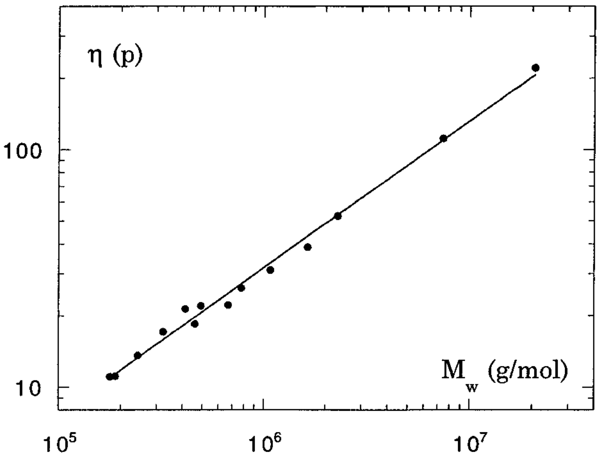

Figure 9. Zero shear viscosity η as a function of the weight average molecular weight M_w (in log–log scale). The power law behavior corresponds to $\eta \propto M_w^{s/\gamma}$ with s/γ = 0.62 (cf. eq 25) leading to $s = 1.1 \pm 0.06$.

Taking γ = 1.74, the value expected from percolation theory (cf. eq 5), one obtains $s = 1.1 \pm 0.06$ for the viscosity divergence exponent value. This exponent lies between the two predicted values: Rouse (s = 4/3) and electrical analogy (s = 0.75). Very recently,[26] it was determined that s = 1.16 and 1.19 for two sets of samples of polybutadiene (M_w = 18 000 and 38 000, respectively) randomly cross-linked at the pendant 1,2 units along the backbone.

3.2.2. Time Dependent Relaxation Spectra. Only the two samples with the largest weight average molecular weights ($M_w = 7.43 \times 10^6$ and 2.06×10^7) have a measurable time dependent relaxation spectra. This is due to the instrument short time limitation, which is of the order of 5 ms. In Figure 10a, the time dependent viscosity[27] η(t) measured for these two samples is shown. In Figure 10b the time dependent viscosity reduced by the zero shear steady viscosity $\eta(t)/\eta$ is plotted. The curves in Figure10a are better described by a logarithmic time function than by a power law. This indicates that the long time cutoff of the power law behavior extends over several time decades including the entire experimentally accessible time window. This also explains the molecular weight dependence of the reduced relaxation spectra $\eta(t)/\eta$ (see Figure 10b). One has to note that η(t) as well as η are measured quantities. However, the two spectra corresponding to the two different molecular weights can be superimposed by using a reduced time scale t/**t*** where **t***, as before, is the relaxation time of the largest cluster in the system. This is shown in Figure 11 in which **t*** is taken to be proportional to M_w^Y where the value of the exponent Y is determined by superposition of the two curves. It is found to be equal to

$$Y = (s + t)/\gamma = 1.75 \pm 0.05 \qquad (26)$$

One has to note that the value for Y corresponding to the Rouse model (Y = 2.3) cannot describe properly the observed relaxation spectra. This is demonstrated by the fact that when using the Rouse value for Y the reduced spectra fail to overlap and remain molecular weight dependent, as shown in the inset of Figure 11.

3.2.3. Frequency-Dependent Relaxation Spectra. On all the samples for which the mean weight average molecular weight has been determined, the imaginary G'' and the real G' parts of the elastic modulus were measured at 25 °C. In the frequency range $0.3 < \omega(\text{Hz}) < 40$, the ratio of these two modulii,

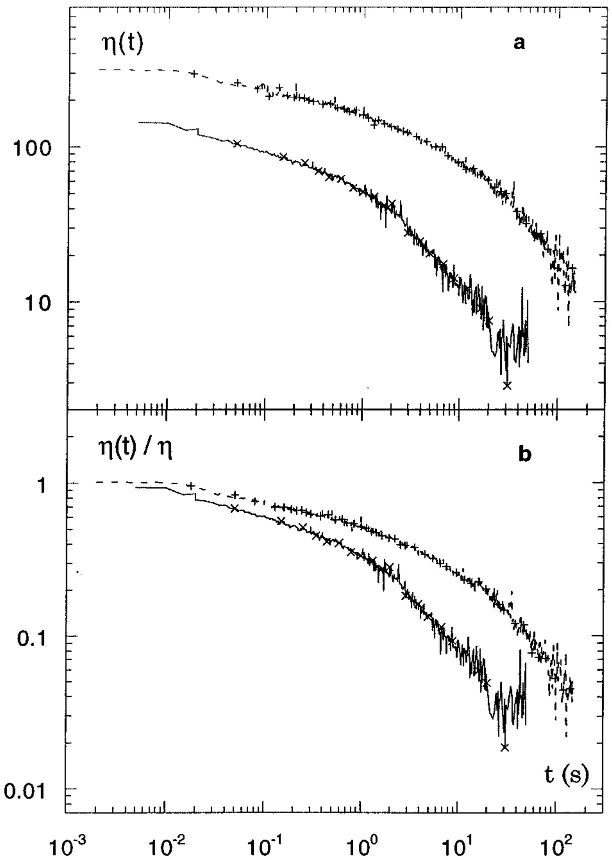

Figure 10. Stress relaxation spectra: (a) time dependent viscosity $\eta(t)$ (in poise) measured on the two samples with the highest molecular masses [(dotted line) $M_w = 2.06 \times 10^7$ (full line) $M_w = 7.43 \times 10^6$)]. The relaxation is not a power law, only the crossover corresponding to the long time cutoff is experimentally accessible. (b) The reduced relaxation spectra $\eta(t)/\eta$ are dependent on the weight average molecular weight.

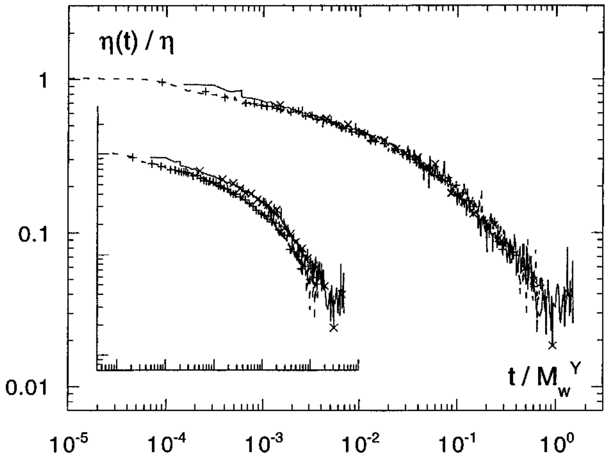

Figure 11. In order to superimpose the two reduced time dependent relaxation spectra $\eta(t)/\eta$, the time axis is divided by the longest relaxation time $\mathbf{t}^*$, which is taken equal to $M_w{}^Y$ (t in s). The exponent Y corresponding to $(s + t)/\gamma$ is adjusted in order to obtain the best data superposition. One finds $Y = 1.75$. In the inset, the use of the Rouse exponent value ($Y = 2.3$) does not allow data superposition.

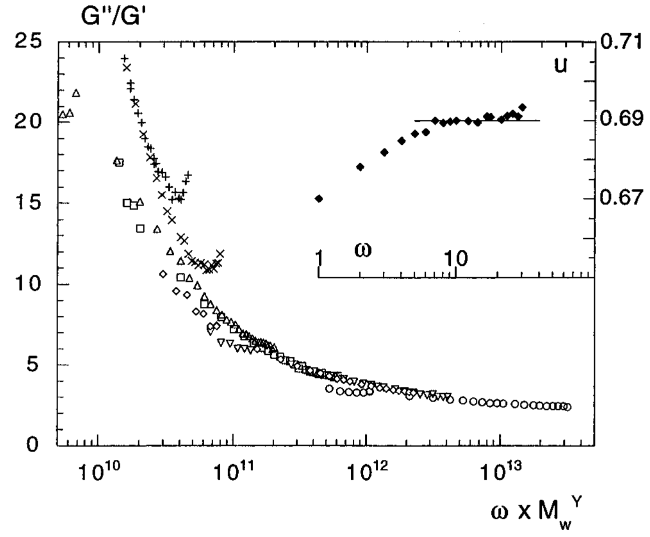

Figure 12. Variation of the loss tangent ($\tan \delta = G''/G'$) as a function of the reduced frequency $\omega\mathbf{t}^*$. The longest relaxation time $\mathbf{t}^*$ is taken equal to $M_w{}^Y$, with Y fixed at the value determined by time-dependent relaxation superposition (with ω in Hz). In the inset the exponent u ($=2/\pi \tan^{-1}(\delta)$) measured on one postgel sample is depicted as a function of the frequency. The full line corresponds to the mean value $u = 0.69$ measured at $7 < \omega$ (Hz) < 30. Different symbols, ○, ∇, ◇, □, △, ×, +, correspond to different molecular weights $M_w \times 10^{-5}$: 74.3, 22.9, 16.4, 7.76, 4.14, 2.43, 1.89.

corresponding to the loss angle δ ($\tan \delta = G''/G'$), is found to be always frequency- and molecular-weight dependent. It indicates that, as for the time dependent relaxation, the accessible frequency window is such that $\omega\mathbf{t}^* < 1$. In order to superimpose the curves obtained for each sample, the frequency is reduced by $\mathbf{t}^* \propto M_w{}^Y$, where Y is taken equal to 1.75, the exponent value determined by the time relaxation superposition (see Figure 11). One may see in Figure 12 that the superposition is correct for the entire set of molecular masses ($1.9 \times 10^5 < M_w < 7.4 \times 10^6$), except for the lower frequency values.[28] On one sample which was synthesized above the gel point (that is, no molecular mass can be measured) there exists a finite range of frequencies ($7 < \omega$ (Hz) < 30) for which the ratio of the two modulii is frequency independent: $\tan(\delta) = G''/G' = 1.91 \pm 0.01$. Thus, in this frequency domain an exponent u can be determined (see the inset in Figure 12):

$$u = 0.69 \pm 0.005 \qquad (27)$$

In Figure 13, the scaling form of the frequency-dependent relaxation spectra (cf eq 10) is depicted. The measured modulii are divided by $G \sim M_w{}^{-t/\gamma}$. Since we have determined experimentally that $s/\gamma = 0.62$ (eq 25) and $Y = (s + t)/\gamma = 1.75$ (eq 26), it follows that $t/\gamma = 1.13$ should be used. The frequency-dependent relaxation is reduced as before, by the characteristic time $\mathbf{t}^* \propto M_w{}^Y$. The successful superposition of the frequency-dependent relaxation data for the entire set of samples based only on the two exponent values separately determined from the time superposition of two samples ($s + t/\gamma$) and from the zero shear viscosity$-M_w$ relation for the entire set of samples (s/γ) proves that these two exponent values are robust.

3.2.4. Dynamic Exponent Values.

We have measured independently three exponent values related to the dynamic properties of the polymer clusters: s/γ (eq 25), $Y = (s + t)/\gamma$ (eq 26), and u (eq 27). Since it is not possible to verify scaling laws directly for time- and frequency-dependent relaxation spectra, let us examine the coherence between exponent values. Using for γ the percolation value 1.74 (eq 5), eq 25 leads to $s = 1.1 \pm 0.06$, eqs 25 and 26 lead to $t/\gamma = 1.1 \pm 0.08$ and thus to $t = 1.9 \pm 0.15$. In recent work on polybutadiene[26] a value of $t = 1.97$ was established for the high-M_w precursor and 2.39 for the low one. We may now

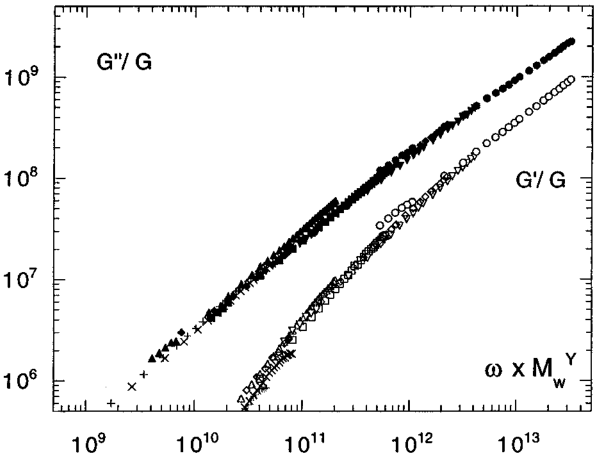

Figure 13. Reduced frequency-dependent dynamic shear modulii: (upper curve) imaginary part G'' (filled symbols); (lower curve) real part G' (empty symbols) of the modulus divided by $G \propto \epsilon^t \propto M_w^{-(Y-s/\gamma)}$. The frequency is reduced by the characteristic time $\mathbf{t}^* \propto M_w^Y$. The exponent values Y and s/γ are taken equal to the values determined by the time dependent relaxation superposition (eq 26) and by the molecular weight dependence of the viscosity (eq 25). One has to note that the numerical factors in the relations linking G and $\mathbf{t}^*$ to M_w are taken equal to 1. Symbols have the same meaning as in Figure 12. Modulii are in dynes/cm^2.

compute $u = t/(s + t) = 0.65 \pm 0.03$. This value has to be compared to the value directly measured on the postgel sample (eq 27): $u = 0.69 \pm 0.005$. As this latter exponent is measured on a single sample, it is free of problems due to local dynamics evolving with the degree of connectivity. This difference between the u exponent values determined on one sample or on the whole set of samples could be due to either an underestimate of experimental precision or due to the effect of solvent neglected in the evaluation of the factor A in eq 24. If one takes into consideration the dependence of the viscosity on molecular weight, the exponent s/γ turns out to be slightly dependent on the diluent concentration.[25] Over a finite range of molecular weight ($2.8 \times 10^5 < M_w < 1.6 \times 10^6$), s/γ decreases from 0.6 at $w = 1$ to 0.5 at $w = 0.6$, and remains unchanged ($s/\gamma = 0.5$) when further diluting from $w = 0.6$ to $w = 0.5$. Taking this value for s/γ and $u = 0.69$ still leaves the value for t unmodified ($t = 1.9$).

The slight concentration dependence of local dynamic properties is a puzzling result. As they are independent of the temperature, an evolution of the glass transition temperature with the degree[29] of connectivity cannot be invoked. In our opinion, this dependence could be related to the progressive depletion of monomers being incorporated into the growing cluster. This disapearance will result in an increase of the local viscosity η_0 and a decrease of the local frequency ω_0, while the local elastic modulus G_0 ($=\eta_0\omega_0$) remains constant. As solvent is added to the samples, the local viscosity changed from η_0 to the solvent viscosity η_s independent of the amount of monomer present. Then, experiments can be compared to the percolation theory in which the number of monomers remains independent of the distance to the gel point.

Conclusion

The static properties of branched poly(dimethylsiloxane) polymers quenched in the proximity of the gelation threshold are well described by the percolation model. Actually, the two exponent values determined in relation to these properties indicate that the gelation of this chemical system belongs to the same universality class as percolation. This system presents the advantage of having local dynamic properties independent of distance to the threshold. Consequently, variation of the zero shear viscosity with the weight average molecular weight is found independent of the temperature and of the diluent concentration, allowing the "real" exponent value to be determined, unlike other chemical systems such as polyurethane.[4] From the data we determine $s/\gamma = 0.62 \pm 0.03$ leading to $s = 1.1 \pm 0.06$. As for the mass dependence of the stress relaxation curve, it leads to $(s + t)/\gamma = 1.75 \pm 0.05$ and to $t = 1.9 \pm 0.15$. These two exponent values are similar to those measured in the case of physical gels which usually correspond to semidilute solutions of connected polymers. In that case the local dynamics are governed by the solvent properties and are independent of the relative distance to the gel point. In fact, the mean values determined on three different physical gels are $s = 0.9 \pm 0.1$ and $t = 1.9 \pm 0.02$ (see Table 4, ref 3). This result confirms that nonconstant local properties play an important role in the determination of the critical exponents for dynamic properties. Finally, we have shown in this paper that polymer clusters undergo hydrodynamic interactions in the reaction bath (i.e., in the undiluted state) as well as in dilute solution.

Acknowledgment. M.G. is grateful for the financial support of the Israel Science Foundation administered by the Israel Academy of Sciences and Humanities. We also wish to acknowledge the help of Y. Yagen and R. Porat in sample preparation. M.A. and D.L. would like to thank M. Daoud and E. Raspaud for helpful discussions.

References and Notes

(1) de Gennes, P. G. *J. Phys. Lett. (Paris)* **1976**, *37*, L1.
(2) Stauffer, D. *J. Chem. Soc., Faraday Trans. 2* **1976**, *72*, 1354.
(3) Adam, M.; Lairez, D. In *Physical Properties of Polymeric Gels*; Cohen Addad, J. P., Ed.; J. Wiley & Sons: Chichester, U.K., 1996; pp 87–142.
(4) Lairez, D.; Adam, M.; Raspaud, E.; Emery, J. R.; Durand, D. *Prog. Colloid Polym. Sci.* **1992**, *42*, 37.
(5) Daoud, M.; Lapp, A. *J. Phys. Condens. Matter* **1990**, *2*, 4021.
(6) In dilute solution, polymer concentration C is much smaller than the overlap concentration C^*.
(7) Using eqs 1 and 3 one finds

$$R_{gz}^{\ 2} = \frac{(3-\tau)}{(3-\tau+2/D)} R_g^{*2} \qquad \text{and} \qquad R_{Hz} = \frac{(3-\tau-1/D)}{(3-\tau)} R_H^*$$

where $\sqrt{R_g^{*2}}$ and R_H^* are the radii of the largest cluster.
(8) Daoud, M.; Leibler, L. *Macromolecules* **1988**, *21*, 1497.
(9) Daoud, M. *J. Phys. Lett. (Paris)* **1984**, *45*, L199.
(10) Stanley, H. E. in *Introduction to Phase Transitions and Critical Phenomena*; Clarendon Press: Oxford, U.K., 1971.
(11) Efros, A. L.; Shklovskii, B. J. P. *Phys. Status Solidi B* **1976**, *76*, 475.
(12) See, for example: Martin, J. E.; Adolf, D.; Wilcoxon, J. P. *Phys. Rev. A* **1989**, *39*, 1325. Rubinstein, M.; Colby, R. H.; Gillmor, J. R. In *Space-Time Organization in Macromolecular Fluids*; Tanaka, F., Doi, M., Ohta T., Eds.; Springer: Berlin, 1989.
(13) de Gennes, P. G. *Scaling Concept in Polymer Physics*; Cornell University Press: Ithaca, NY 1979.
(14) See, for example: Gottlieb, M.; Macosko, C. W.; Benjamin, G. S.; Meyers, K. O.; Merrill, E. W. *Macromolecules* **1981**, *14*, 1039. Gottlieb, M.; Macosko, C. W.; Lepsch, T. C. *J. Polym.*

Sci., Polym. Phys. Ed. **1981**, *19*, 1603. Venkataraman, S. K.; Coyne, L.; Chambon, F.; Gottlieb, M.; Winter, H. H. *Polym. Prepr. (Am. Chem. Soc., Div. Polym. Chem.)* **1988**, *29*, 571. Venkataraman, S. K.; Coyne, L.; Chambon, F.; Gottlieb, M.; Winter, H. H. *Polymer* **1989**, *30*, 2222. Shefer, A.; Gottlieb, M. *Macromolecules* **1992**, *25*, 4036.

(15) Luzzati, S.; Adam, M.; Delsanti, M. *Polymer* **1986**, *27*, 834. Adam, M.; Delsanti, M.; Munch, J.-P.; Durand, D. *J. Phys.* **1987**, *48*, 1809.

(16) Bouchaud, E.; Delsanti, M.; Adam, M.; Daoud, M.; Durand, D. *J. Phys.* **1986**, *47*, 1273.

(17) Delsanti, M. Thesis, Université de Paris Sud, France, 1978.

(18) Weill, G.; des Cloizeaux, J. *J. Phys.* **1979**, *40*, 99.

(19) Oono, Y. *J. Chem. Phys.* **1983**, *79*, 4629.

(20) Adam, M.; Delsanti, M.; Pieransky, P. *Rev. Phys. Appl. Fr.* **1984**, *19*, 253.

(21) Doi, M.; Edwards, S. F. In *The Theory of Polymer Dynamics*; Clarendon Press: Oxford, U.K., 1986; p 135.

(22) Adam, M.; Lairez, D.; Raspaud, E.; Farago, B. *Phys. Rev. Lett.* **1996**, *77*, 3673.

(23) Lapp, A.; Leibler, L.; Schosseler, F.; Strazielle, C. *Macromolecules* **1989**, *22*, 2871.

(24) Phillies, G. D. J. *J. Phys. Chem.* **1992**, *96*, 10061.

(25) In fact the slight concentration dependence of the factor A in eq 24 implies a small concentration dependence of the exponent s/γ, which varies between 0.6 and 0.5 as the concentration decreases. The value 0.62 measured in the bulk is thus an upper limit.

(26) Mours, M.; Winter, H. H. *Macromolecules* **1996**, *29*, 7221.

(27) In the following, η stands for $\eta(M_w,T,w)$ with $T = 8$ °C and $w = 1$ g/g.

(28) This departure from a single curve may be due to the lack of precision at low frequency, that is when the moduli are smaller than a few dynes/cm$^{2.}$

(29) This could appear in contradiction with: Shefer, A.; Gottlieb, M. *Macromolecules* **1992**, *25*, 4036. However, due to the limited range of stoichiometric ratio r studied here, ($|r - r_c| < 0.05$), with r_c the r value at the gel point) one can deduce from this reference that T_g varies at most by a one-third of a degree.

MA970184A